Asian Journal of Chemistry; Vol. 34, No. 7 (2022), 1835-1840

ASIAN JOURNAL OF CHEMISTRY

https://doi.org/10.14233/ajchem.2022.23844

Influence of Different Synthetic Methods on Morphology and Luminescent Properties of $LaF_3:Eu^{3+}$ Nanoparticles

J. LADOL

Department of Chemistry, Government Degree College, Nobra-194401, India

Corresponding author: E-mail: jigmetladol789@gmail.com

Received: 22 March 2022; *Accepted*: 4 May 2022; *Published online*: 15 June 2022; AJC-20863

Fluorescent europium ion doped lanthanum fluoride ($LaF_3:Eu^{3+}$) nanoparticles were synthesized using various methods which includes hydrothermal, co-precipitation and sonochemical method. A series of experiments were performed to obtain variations in the morphology, structure and optical behaviour of fabricated products. The optical and structural properties of the fabricated nanoparticles (NPs) were characterized through scanning electron microscopy (SEM), powder X-ray diffraction (PXRD), energy dispersive X-ray spectroscopy (EDS), Fourier transform infrared (FTIR) spectrometry, and particle size by dynamic light scattering (DLS). In LaF_3 nanoparticles, the existence of europium as dopant ions was confirmed through energy dispersive X-ray spectroscopy (EDS). The optical properties of the synthesized nanoparticles were investigated by conducting photoluminescence (PL) studies.

Keywords: Nanoparticles, Fluorides, Photoluminescence, X-ray diffraction, Infrared spectroscopy.

INTRODUCTION

Trivalent lanthanide nanomaterials, doped with other lanthanide ion, of nanoscale and microscale inorganic materials having advanced functions and special hierarchical architectures have received considerable attention for their promising applications in various fields, including three-dimensional displays, photo-dynamic therapy, catalysis, low-intensity IR imaging, solid-state lasers and other optical devices obtained from intra *f-f* transitions [1-5]. Considerable research attention has been given to the lanthanide ions due to their characteristic electronic and optical properties, including long-lived emissions, high luminescence quantum yields, narrow bandwidths and large Stokes shifts resulting from the 4*f*-4*f* and 4*f*-5*d* electronic transitions [6,7]. With their luminescent characteristics, lanthanide ions are applied as dopants in electroluminescent devices [8], tele-communication [9], bioanalytical sensors [10], solar cells [11] and bioimaging set-ups [12]. Among different host materials used for a trivalent lanthanide ion, lanthanide fluorides are the optimum host lattices because of their low phonon energies and high thermochemical stability to reduce non-radiative relaxations, which improves the luminescence of optically active dopants [13-17]. For efficient luminescence, high ionicity and low-energy phonons are the most preferred properties. The formation and co-doping of core-shell nanoparticles [18,19] by using another rare-earth ion at low-doping concentrations [20,21] result in sustainable modifications in down-conversion (DC) emission spectra by varying the local environment. However, the crystal phase remains the same. Moreover, nano-structured materials luminescence efficiency is lower than corresponding bulk phosphors luminescence efficiency due to nonradiative decay caused by defects on the nanoparticle surface. To lower such a defect, the lanthanide-doped luminescent materials of various structures have been fabricated using different techniques, such as co-precipitation [22], thermal decomposition [23], hydrothermal [24-27], microemulsion-assisted synthesis [28], ionic liquid-based synthesis [29,30], and microwave-assisted synthesis [31].

In this study, the Eu^{3+} ion doped lanthanum fluoride nanoparticles with various morphologies were synthesised using the co-precipitation, hydrothermal, and sonochemical methods. Among these techniques, hydrothermal synthesis allowed excellent control over the particle shape, size and distribution and material crystallinity. The luminescent efficiency of Eu^{3+} doped lanthanum fluoride (LaF_3) nanoparticles was studied. These nanoparticles are favourable to be used as luminescent probes in imaging technology and biological labeling.

EXPERIMENTAL

The chemicals *viz*. lanthanum nitrate hexahydrate $La(NO_3)_3 \cdot 6H_2O$ (99.9%), europium nitrate hexahydrate $Eu(NO_3)_3 \cdot 6H_2O$ (99.9%) and ammonium tetrafluoroborate (NH_4BF_4) were procured from Alfa Aesar. Other chemicals, including sodium hydroxide, citric acid and ethanol, were of analytical grade. All the chemicals were used as obtained without further purification. Deionized water was used.

Synthesis of $LaF_3:Eu^{3+}$ nanoparticles

Hydrothermal method: For the preparation of Eu^{3+} doped LaF_3 nanoparticles, an aqueous solution (4 mL) of $Eu(NO_3)_3 \cdot 6H_2O$ (0.2 mmol, 0.09 g) and $La(NO_3)_3 \cdot 6H_2O$ (0.8 mmol, 0.35 g) was mixed with 10 mL of citric acid (1 mmol, 0.2 g) with thorough stirring. To this reaction solution, 10 mL of NH_4BF_4 (2 mmol, 0.20 g) was added dropwise. After vigorously stirring this solution at room temperature for 30 min, the colloidal solution was transferred into a 20 mL Teflon-lined autoclave. The autoclave was sealed and heated at 180 ºC for 24 h. The autoclave was allowed to naturally cool down to room temperature. The precipitate was separated through centrifugation and then, sequentially washed with deionized water and ethanol. Finally, the collected nanoparticles were dried at 60 ºC for 12 h.

Co-precipitation method: $LaF_3:Eu^{3+}$ nanoparticles were prepared using co-precipitation, where citric acid (2 mmol; 0.4 g) and NH_4BF_4 (4 mmol; 0.40 g) were mixed in the molar ratio of 1:2. This mixture was dissolved in 45 mL of deionized water. The solution pH was adjusted to 6 by adding aqueous ammonia and then the resulting solution was heated to 75 ºC. $Eu(NO_3)_3 \cdot 6H_2O$ (0.2 g; 0.4 mmol) and $La(NO_3)_3 \cdot 6H_2O$ (0.70 g; 1.6 mmol) were dissolved in 5 mL of deionized water and this solution was added dropwise in the aforementioned solution. A white precipitate formed and dissolved after a few seconds, providing a clear solution. After 20 h of reaction, the reaction mixture was cooled down to room temperature. Then, 70 mL of ethanol was added to the reaction mixture for precipitation of the nanoparticles, which were collected through centrifugation, sequentially washed with deionized water and ethanol and finally were dried at 60 ºC for 12 h.

Sonochemical method: Eu^{3+} doped LaF_3 nanoparticles were prepared by introducing 2 mmol citric acid (0.4 g) into 30 mL of distilled water. Then, $Eu(NO_3)_3 \cdot 6H_2O$ (0.2 g, 0.4 mmol) and $La(NO_3)_3 \cdot 6H_2O$ (0.70 g, 1.6 mmol) were added to this solution with continuous stirring. Into the resulting reaction mixture, 10 mL of aqueous NH_4BF_4 (4 mmol, 0.40 g) was added dropwise. Subsequently, this mixture solution was subjected to high-intensity ultrasound irradiation for 8 h in ambient air. Ultrasound irradiation was produced with a high-intensity ultrasonic probe directly immersed in the reaction solution. At the end of reactions, a large amount of white precipitate was obtained. After the precipitate cooled to room temperature, it was centrifuged, sequentially washed with distilled water, absolute ethanol and acetone, and dried at room temperature in the air.

Spectroscopic and microscopic measurements: The size and phase structure of the as-fabricated samples were characterized through PXRD by using the D8 X-ray diffractometer (Bruker) at the 2θ of 10º-70º and a scanning rate of 12º min^{-1} with Cu*K*α radiation (λ = 0.15405 nm). At an accelerating voltage of 5 kV, the SEM images of the samples were obtained on FEI Nova SEM 450. The energy spectra were obtained through EDS (Oxford Instrument). The infrared spectra were recorded on the Shimadzu Fourier transform infrared spectrometer (FT-IR) in 4000-400 cm^{-1}. The standard KBr pellet method was used. The photoluminescence emission and excitation spectra were recorded using Agilent Cary Eclipse fluorescence spectrophotometer with a xenon lamp used as the excitation source at room temperature. The radiative lifetimes of luminescent nanoparticles were determined from the decay curves by using picosecond time-resolved cum steady state luminescence spectrometer, Eddinburg Instruments, Model: FSP920. All the analyses were conducted at room temperature.

RESULTS AND DISCUSSION

PXRD measurements: The crystallinity and phase of the as-fabricated samples were estimated using PXRD patterns (Fig. 1). The PXRD patterns of the nanoparticles indicated that their intensities and peak positions strongly agreed with those reported in the JCPDS standard card No. 32-048 [32] for the hexagonal-phase LaF_3 nanoparticles. The hexagonal LaF_3 phase showing diffraction peaks at 24.4º, 27.8º, 35.2º, 43.9º, 52.7º and 64.5º can be indexed to the planes (002), (111), (112), (300), (221) and (223), respectively. The broadening of diffraction peaks indicated the nanoscale sizes of the prepared doped LaF_3 nanoparticles using different methods. The average crystallite size of these nanospheres was estimated by using the modified Scherrer's equation:

$$\ln\beta\,(^\circ) = \frac{\ln K\lambda\,(\text{nm})}{L\,(\text{nm})} + \ln\frac{1}{\cos\theta\,(^\circ)}$$

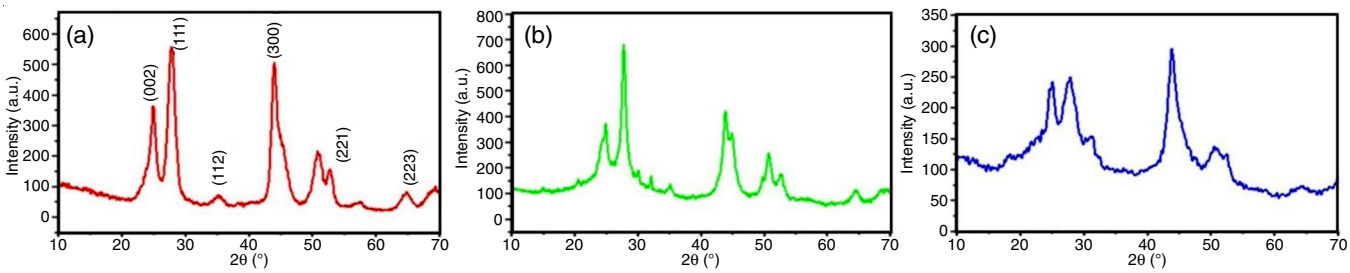

Fig. 1. PXRD patterns for $LaF_3:Eu^{3+}$ nanoparticles (a) hydrothermal, (b) co-precipitation, (c) sonochemical method

where, L is the crystallite size, λ is the wavelength of the Cu Kα radiant, λ = 0.15405 nm, β is the full-width at half-maximum (fwhm) of the diffraction peak, θ is the diffraction angle and K is the Scherrer constant equals to 0.89. The plot of ln β *versus* ln 1/cos θ is a straight line with the intercept of ln Kλ/L and slope of approximately 1. When the intercept was obtained, the intercept exponential was acquired. After getting the intercept, then the exponential of the intercept was obtained:

$$e^{\ln K\lambda/L} = \frac{K\lambda\ (nm)}{L\ (nm)}$$

Using the values of λ and K, a single value of L was calculated in nanometer. All the major peaks were employed to compute the average crystallite size of LaF_3 nanoparticles. The improved peak intensities indicated the preferential crystal growth in a particular direction. The estimated average sizes of crystallite were 29, 24 and 36 nm for the prepared LaF_3 nanoparticles using coprecipitation, hydrothermal and sonochemical methods, respectively.

To distinguish the effects of the strain and crystallite size on induced broadening, the Williamson-Hall plots of XRD peaks were obtained. The strain and crystallite size can be obtained using the *y*-axis intercept and line slope, respectively, with the following equation:

$$\beta_{hkl}\cos\theta = \frac{k\lambda}{L} + 4\varepsilon\sin\theta$$

where β is the full-width at half-maximum of the diffraction peak in radian, L is the crystallite size in nm, ε is the strain, and λ is X-ray wavelength in nm. The grain size of 14, 17 and 28 nm and grain strain of 2.5×10^{-3}, 8.77×10^{-4} and 1.15×10^{-3} have been calculated for LaF_3 nanoparticles synthesized by hydrothermal, co-precipitation and sonochemical methods, respectively. The corresponding Williamson-Hall plots are shown in Fig. 2.

SEM and EDS studies: The surface morphology of the Eu^{3+} doped LaF_3 nanoparticles was explored from scanning electron micrographs (SEM). Fig. 3a shows a well dispersed particles having a pseudo-spherical shaped morphology synthesized by hydrothermal method. Fig. 3b show aggregated porous nanomaterials synthesized by co-precipitation method whereas by sonochemical method (Fig. 3c), the product has

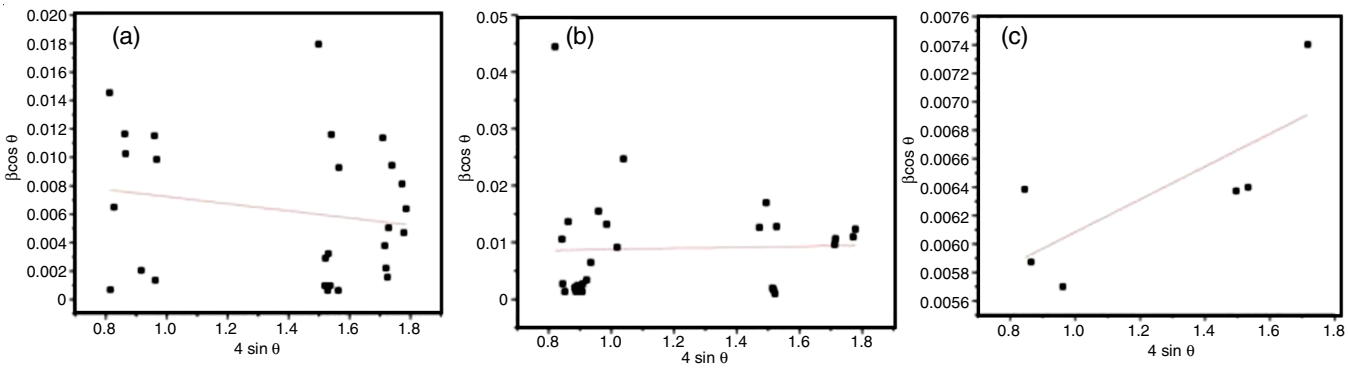

Fig. 2. Williamson Hall plots for $LaF_3:Eu^{3+}$ nanoparticles: (a) hydrothermal, (b) co-precipitation, (c) sonochemical method

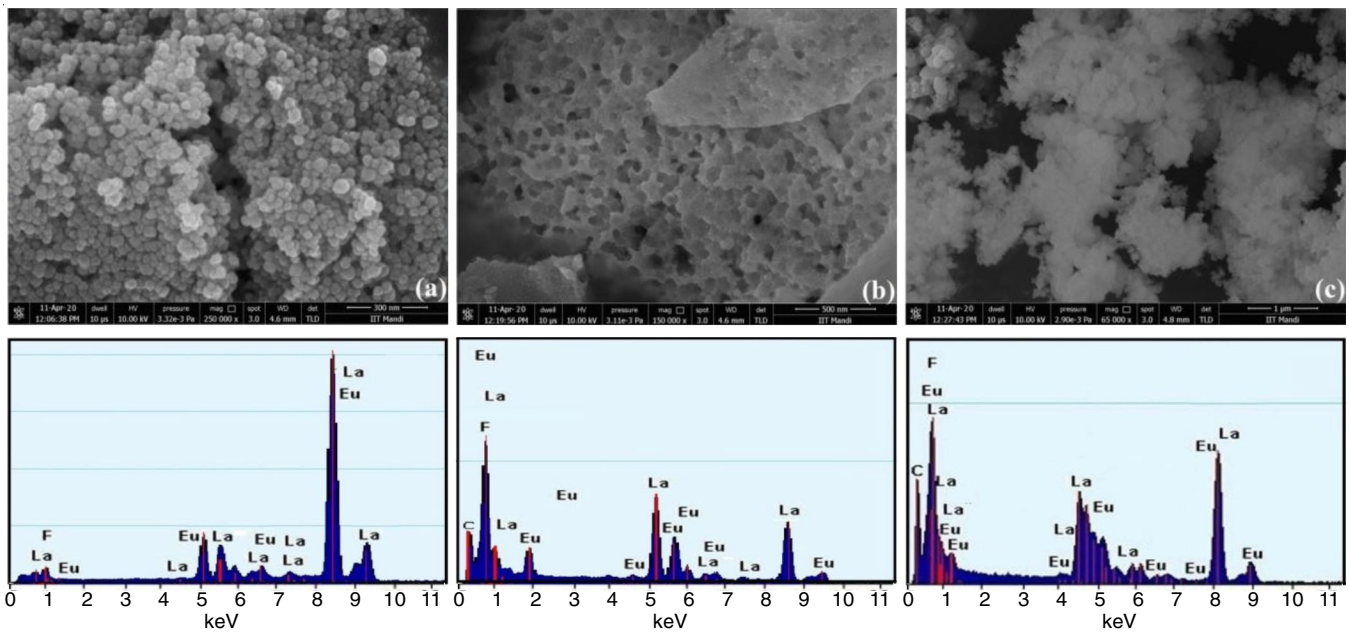

Fig. 3. SEM images and EDS spectrum of $LaF_3:Eu^{3+}$ nanoparticles synthesized by (a) hydrothermal method, (b) co-precipitation, (c) sonochemical method

aggregated pseudo-spherical shaped morphology. Compositional analysis by energy dispersive X-ray spectroscopy (EDS) revealed incorporation of Eu^{3+} ions in host LaF_3 nanoparticles by hydrothermal, co-precipitation and sonochemical methods.

Particle size by DLS technique: The size of as-prepared particles in colloidal state was determined by dispersing the products in an aqueous medium through 15 min ultrasonication. The obtained particle sizes are displayed in Fig. 4. The mean particle sizes of 54, 40 and 62 nm were observed for prepared Eu^{3+} doped LaF_3 nanoparticles using co-precipitation, hydrothermal, and sonochemical methods, respectively. The particle sizes acquired from this method are larger than those obtained from the PXRD data because of the shape effects and surface solvation of nanoparticles.

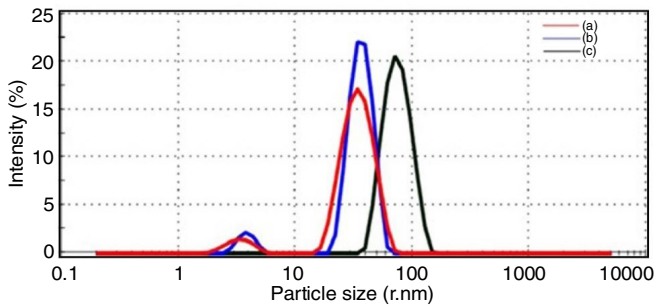

Fig. 4. Particle size by DLS technique for $LaF_3:Eu^{3+}$ nanoparticles (a) hydrothermal, (b) coprecipitation, (c) sonochemical method

FTIR spectra: Studies shown by FTIR confirm the presence of citrate ligands at the surface of $LaF_3:Eu^{3+}$ nanoparticles (Fig. 5). The characteristic band at 3449 cm^{-1} can be assigned to the stretching mode of hydrogen bonded hydroxyl groups. Whereas, the bands at 2886 and 2828 cm^{-1} appear due to the asymmetrical and symmetrical stretching vibration modes of CH_2 group. The bands at 1581 and 1384 cm^{-1} can be attributed to the asymmetrical and symmetrical stretching vibration modes of the carboxylate group, respectively.

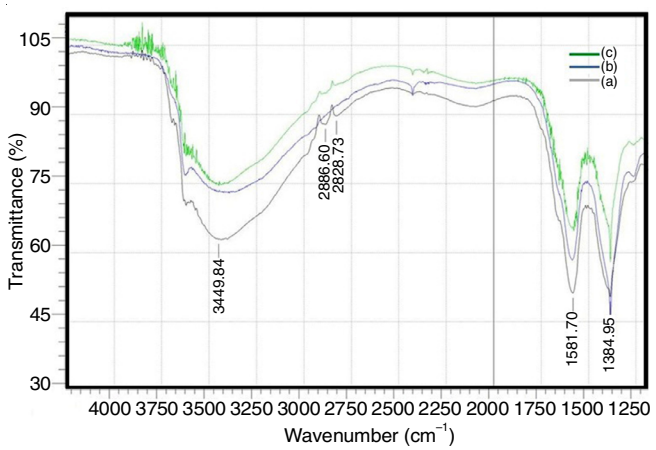

Fig. 5. FTIR spectra of $LaF_3:Eu^{3+}$ nanoparticles synthesized by (a) hydrothermal method, (b) coprecipitation, (c) sonochemical method

Down-conversion photoluminescence: Fig. 6 shows the excitation and emission spectra for $LaF_3:Eu^{3+}$ nanoparticles

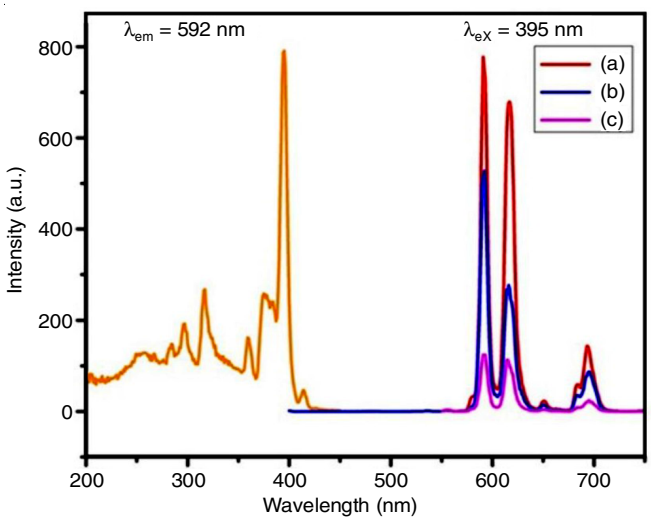

Fig. 6. Excitation and emission spectra of $LaF_3:Eu^{3+}$ nanoparticles monitored at λ_{em} = 592 nm and λ_{ex} = 395 nm: (a) hydrothermal, (b) co-precipitation, (c) sonochemical method

synthesized using the hydrothermal, co-precipitation and sonochemical methods. The excitation spectrum consists of several characteristic excitation lines of Eu^{3+} originating due to the *f-f* transitions within the 4*f* Eu^{3+} ions. The prominent emission peak at 395 nm originates from $^7F_0 \rightarrow {}^5L_6$ transition. Upon excitation at 395 nm, the corresponding emission spectrum comprises emission lines assigned at 592 nm: $^5D_0 \rightarrow {}^7F_1$; 615 nm: $^5D_0 \rightarrow {}^7F_2$; 650 nm: $^5D_0 \rightarrow {}^7F_3$ and 695 nm: $^5D_0 \rightarrow {}^7F_4$. Though the emission spectrum of all the synthesized nanoparticles was same yet the difference lies in the peak intensity. The $LaF_3:Eu^{3+}$ nanoparticles synthesized by hydrothermal method possess enhanced emission intensity than that observed for synthesized nanoparticles by co-precipitation and sonochemical methods. It is observed that $^5D_0 \rightarrow {}^7F_1$ magnetic-dipole transition is the strongest in the three samples, indicating that the Eu^{3+} ion is located in the LaF_3 crystal sites with an inversion centre. The luminescence decay curves of Eu^{3+} in LaF_3 nanoparticles were measured and compared.

Fig. 7a-c show the luminescence dynamics of Eu^{3+} in LaF_3 nanoparticles. The lifetimes of Eu^{3+} synthesized by hydrothermal, co-precipitation and sonochemical methods in $LaF_3:Eu^{3+}$ nanoparticles were 7.453, 6.415 and 4.822 ns respectively, (Table-1). The difference in luminescence intensity of $LaF_3:Eu^{3+}$ nanoparticles synthesized using different techniques is associated with best crystallinity and morphology as analyzed from their PXRD patterns and SEM images.

TABLE-1
LUMINESCENCE RADIATIVE LIFETIMES OF THE $LaF_3:Eu^{3+}$ SAMPLES MONITORED AT λ_{em} = 592 nm AND λ_{ex} = 395 nm

Synthetic method	Lifetime τ (ns)
Hydrothermal	7.453
Sonochemical	6.415
Co-precipitation	4.822

In general, the purity of the substance colour is determined using colour coordinates. Thus, the chromaticity coordinates of Eu^{3+} doped LaF_3 nanoparticles were computed using the

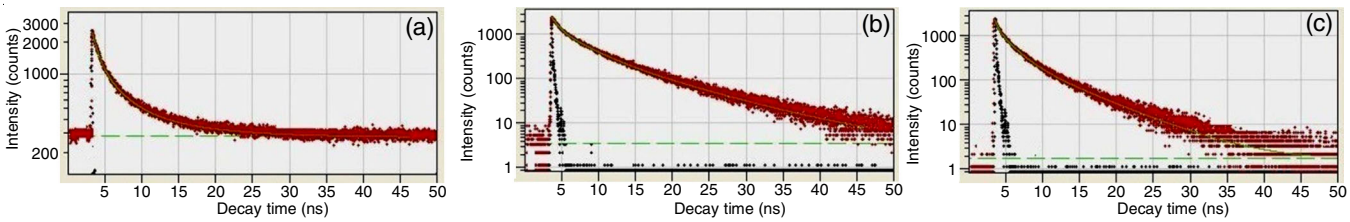

Fig. 7. Decay curve of Eu^{3+} luminescence in $LaF_3:Eu^{3+}$ nanoparticles: (a) hydrothermal, (b) coprecipitation, (c) sonochemical method

emission spectra by employing the Commission Inter-national De l'Eclairage (CIE) system. For $LaF_3:Eu^{3+}$ nano-particles, the CIE chromaticity diagram obtained at 395 nm is presented in Fig. 8. The CIE coordinate was (0.62, 0.39), which is in the red region. Therefore, the prepared $LaF_3:Eu^{3+}$ nano-particles can act as red-colour-producing materials for light emitting diodes and display applications because of their strong emission at 592 nm.

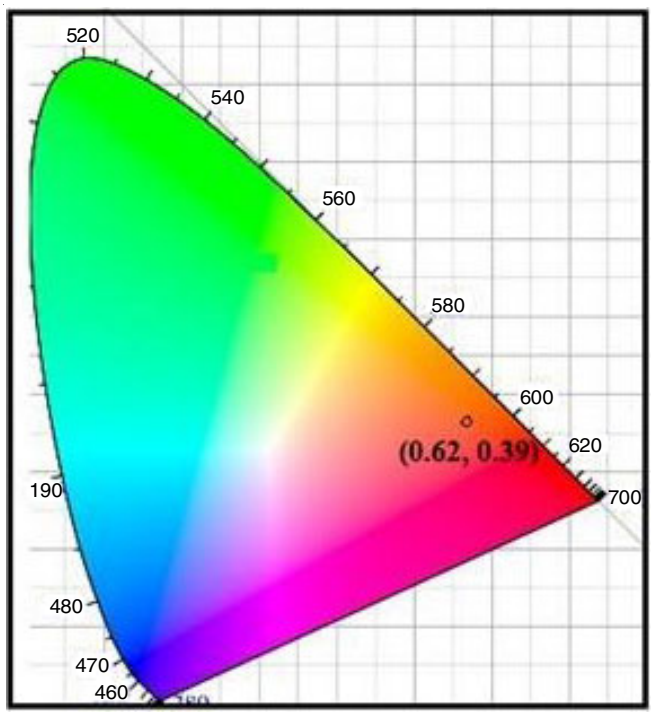

Fig. 8. CIE chromatogram for $LaF_3:Eu^{3+}$ nanoparticles

Conclusion

The $LaF_3:Eu^{3+}$ nanoparticles were successfully prepared using coprecipitation, hydrothermal and sonochemical methods. The PXRD studies revealed the hexagonal phase of prepared $LaF_3:Eu^{3+}$ nanoparticles. The size of the prepared nanoparticles was ranged 14-60 nm. The morphology and phase evolution was explained. The nanoscale particle size of the prepared samples was confirmed through PXRD and DLS. The photo-luminescence studies indicated a general development route for highly-efficient luminescent DC phosphors prepared using the hydrothermal method compared with the nanoparticles prepared using sonochemical and co-precipitation methods. The purity of the nanoparticle colour was confirmed using the colour coordinates. All the synthetic procedures are environmentally friendly, simple and may be applied in the preparation of other materials with submicron morphologies.

ACKNOWLEDGEMENTS

The author acknowledges Indian Institute of Technology Roorkee and Indian Institute of Technology Madras for their technical support. Thanks are also due to SAIF, Panjab University, Chandigarh for powder X-ray diffraction analysis and Dr. Vinay Kumar, School of Physics, Shri Mata Vaishno Devi University, Katra, India for conducting the photoluminescence analysis.

CONFLICT OF INTEREST

The authors declare that there is no conflict of interests regarding the publication of this article.

REFERENCES

1. W. Xu, Y. Wang, X. Bai, B. Dong, Q. Liu, J.S. Chen and H.W. Song, *J. Phys. Chem. C*, **114**, 14018 (2010); https://doi.org/10.1021/jp1048666
2. C.X. Li and J. Lin, *J. Mater. Chem.*, **20**, 6831 (2010); https://doi.org/10.1039/c0jm00031k
3. T. Yu, J. Joo, Y.I. Park and T. Hyeon, *Angew. Chem. Int. Ed.*, **44**, 7411 (2005); https://doi.org/10.1002/anie.200500992
4. H.X. Mai, Y.W. Zhang, R. Si, Z.G. Yan, L.D. Sun, L.P. You and C.H. Yan, *J. Am. Chem. Soc.*, **128**, 6426 (2006); https://doi.org/10.1021/ja060212h
5. M. Yu, H. Wang, C.K. Lin, G.Z. Li and J. Lin, *Nanotechnology*, **17**, 3245 (2006); https://doi.org/10.1088/0957-4484/17/13/028
6. W. Zheng, P. Huang, D. Tu, E. Ma, H. Zhu and X. Chen, *Chem. Soc. Rev.*, **44**, 1379 (2015); https://doi.org/10.1039/C4CS00178H
7. P. Dorenbos, *J. Lumin.*, **134**, 310 (2013); https://doi.org/10.1016/j.jlumin.2012.08.028
8. C.C. Lin and R.S. Liu, *J. Phys. Chem. Lett.*, **2**, 1268 (2011); https://doi.org/10.1021/jz2002452
9. W. Blanc and B. Dussardier, *J. Opt.*, **45**, 247 (2016); https://doi.org/10.1007/s12596-015-0281-6
10. J.B. Liu, X.H. Yang, X.X. He, K.M. Wang, Q. Wang, Q.P. Guo, H. Shi, J. Huang and X.Q. Huo, *Sci. China Chem.*, **54**, 1157 (2011); https://doi.org/10.1007/s11426-011-4350-7
11. Y. Shang, S. Hao, C. Yang and G. Chen, *Nanomaterials*, **5**, 1782 (2015); https://doi.org/10.3390/nano5041782
12. M.V. DaCosta, S. Doughan, Y. Han and U.J. Krull, *Anal. Chim. Acta*, **832**, 1 (2014); https://doi.org/10.1016/j.aca.2014.04.030
13. S. Varun, M. Kalra and M. Gandhi, *J. Fluoresc.*, **25**, 1501 (2015); https://doi.org/10.1007/s10895-015-1641-y
14. H. Khajuria, J. Ladol, S. Khajuria, M.S. Shah and H.N. Sheikh, *Mater. Res. Bull.*, **80**, 150 (2016); https://doi.org/10.1016/j.materresbull.2016.03.022
15. H. Khajuria, J. Ladol, R. Singh, H.N. Sheikh and V. Kumar, *J. Chem. Sci.*, **129**, 753 (2017); https://doi.org/10.1007/s12039-017-1296-0

16. C. Zhang, C. Li, C. Peng, R. Chai, S. Huang, D. Yang, Z. Cheng and J. Lin, *Chem. Eur. J.*, **16**, 5672 (2010); https://doi.org/10.1002/chem.200903137
17. C. Zhang, Z. Hou, R. Chai, Z. Cheng, Z. Xu, C. Li, L. Huang and J. Lin, *J. Phys. Chem. C*, **114**, 6928 (2010); https://doi.org/10.1021/jp911775z
18. C. Li, X. Liu, P. Yang, C. Zhang, H. Lian and J. Lin, *J. Phys. Chem. C*, **112**, 2904 (2008); https://doi.org/10.1021/jp709941p
19. J. Ladol, H. Khajuria, H.N. Sheikh and Y. Khajuria, *J. Chem. Sci.*, **128**, 1149 (2016); https://doi.org/10.1007/s12039-016-1108-y
20. D.L. Gao, H.R. Zheng, X.Y. Zhang, W. Gao, Y. Tian, J. Li and M. Cui, *Nanotechnology*, **22**, 175702 (2011); https://doi.org/10.1088/0957-4484/22/17/175702
21. J. Ladol, H. Khajuria, S. Khajuria and H.N. Sheikh, *Nanochem. Res.*, **2**, 188 (2017); https://doi.org/10.22036/NCR.2017.02.005
22. X. Teng, Y. Zhu, W. Wei, S. Wang, J. Huang, R. Naccache, W. Hu, A.I.Y. Tok, Y. Han, Q. Zhang, Q. Fan, W. Huang, J.A. Capobianco and L. Huang, *J. Am. Chem. Soc.*, **134**, 8340 (2012); https://doi.org/10.1021/ja3016236
23. G.Y. Chen, T.Y. Ohulchanskyy, A. Kachynski, H. Agren and P.N. Prasad, *ACS Nano*, **5**, 4981 (2011); https://doi.org/10.1021/nn201083j
24. M. Shang, G. Li, X. Kang, D. Yang, D. Geng, C. Peng, Z. Cheng, H. Lian and J. Lin, *Dalton Trans.*, **41**, 5571 (2012); https://doi.org/10.1039/c2dt30082f
25. M. Shang, D.L. Geng, X.J. Kang, D.M. Yang, Y. Zhang and J. Lin, *Inorg. Chem.*, **51**, 11106 (2012); https://doi.org/10.1021/ic301662c
26. J. Ladol, H. Khajuria and H.N. Sheikh, *J. Mater. Sci. Mater. Electron.*, **27**, 4084 (2016); https://doi.org/10.1007/s10854-015-4267-6
27. J. Ladol, H. Khajuria, S. Khajuria and H.N. Sheikh, *Bull. Mater. Sci.*, **39**, 943 (2016); https://doi.org/10.1007/s12034-016-1225-8
28. J. Zhou, X.J. Zhu, M. Chen, Y. Sun and F.Y. Li, *Biomaterials*, **33**, 6201 (2012); https://doi.org/10.1016/j.biomaterials.2012.05.036
29. M. He, P. Huang, C.L. Zhang, H.Y. Hu, C.C. Bao, G. Gao, R. He and D.X. Cui, *Adv. Funct. Mater.*, **21**, 4470 (2011); https://doi.org/10.1002/adfm.201101040
30. S. Khajuria, J. Ladol, S. Sanotra and H.N. Sheikh, *Appl. Nanosci.*, **6**, 653 (2016); https://doi.org/10.1007/s13204-015-0478-7
31. F. Li, C. Li, X. Liu, Y. Chen, T. Bai, L. Wang, W. Shi and S. Feng, *Chem. Eur. J.*, **18**, 11641 (2012); https://doi.org/10.1002/chem.201201309
32. F. Wang, Y. Zhang, X. Fan and M. Wang, *J. Mater. Chem.*, **16**, 1031 (2006); https://doi.org/10.1039/b518262j